Nanocrystalline Rare Earth Oxide Coatings for Increased Protection of Iron-chromium Alloys at High Temperatures

Stela M.C.Fernandes, Olandir V.Corea, Lalgudi V.Ramanathan
Instituto de Pesquisas Energéticas e Nucleares
Av. Prof. Lineu Prestes 2242, São Paulo, Brazil
stelamcf@ipen.br;ovcorrea@ipen.br;lalgudi@ipen.br

Abstract- Rare earths have been used to increase high temperature oxidation resistance of chromium dioxide and alumina forming alloys. These rare earths can be added as elements to the alloy or applied as an oxide coating to the alloy surface. The sol-gel technique was used to apply nanocrystalline oxide coatings of a variety of rare earths on Fe-20Cr alloy surfaces. In the first set of experiments the cyclic oxidation behaviour of uncoated and rare earth oxide coated specimens of this alloy was determined. The cyclic oxidation resistance of the alloy varied with the nature of the rare earth and this in turn was influenced by the rare earth ion radius and characteristics of the rare earth oxide coating such as morphology, crystallite size and coverage. The second set of experiments was carried out to optimize the rare earth oxide coatings and consisted in determination of the oxidation behaviour of Fe20Cr and Fe20Cr5Al alloy specimens coated with CeO_2, La_2O_3 and $CeO_2 + La_2O_3$ at 1000 °C. The oxidation resistance of the two alloys coated with a mixture of CeO_2 and La_2O_3 was significantly higher than those coated with either oxide. The role of rare earths and characteristics of the rare earth oxide in increasing oxidation resistance of chromium dioxide forming alloys are also presented.

Keywords: Nanocrystalline, Rare earth oxide, Oxidation, Iron-chromium alloy.

1. Introduction

Alloys for use at high temperatures often rely on the formation of protective layers of chromium dioxide or alumina. The use of reactive elements, mainly rare earths (RE) to improve high temperature oxidation resistance of chromium dioxide and alumina forming alloys is well known. The improvements in oxidation resistance are in the form of reduced oxidation rates and increased oxide scale adhesion as shown previously by Stott (1989) and Stringer (1989). The RE can be added to the alloy as an element or oxide (to form a dispersion) or applied as an oxide coating to the alloy surface as reported by Hou and Stringer (1987) and Ramanathan (1993). Application of RE oxides to metallic surfaces can be achieved by immersion in aqueous nitrate solutions followed by thermal decomposition of the solid nitrate to oxide. Other precursors for RE oxide coatings can be molten nitrate salts or oxide slurries. The RE oxides thus formed on the alloy surface are microcrystalline as reported by Seal et.al (2000). The sol-gel technique can be also used to coat alloy surfaces with RE oxides. Essentially this technique is based on the use of sols, which consists of a stable dispersion in a liquid of colloidal units of hydrous RE oxides or hydroxides. The RE oxide sol is applied to the alloy surface by a suitable technique, such as dipping, spin coating or electrophoresis. On drying, (removing water from the colloidal units) the sol is transformed into a gel of RE oxide ranging in size between 2 and 100 nm as reported by Bennet (1984).

Compared to adding RE elements to the alloy to improve its oxidation resistance, RE oxide coatings do not affect adversely the mechanical properties of the alloy. The oxide coatings can be also used on metallic components in service and exposed to high temperature oxidizing environments. A marked increase in isothermal and cyclic oxidation resistance of Fe-Cr alloys coated with nanocrystalline RE oxides has been observed and reported by Fernandes and Ramanathan (2000, 2006). This increase in oxidation resistance was attributed to a combination of factors that include the ionic radius of the RE and the morphology of the RE oxide. Considering the increasing demand in recent years for even higher oxidation resistance in chromium dioxide and alumina forming alloys, attempts are in progress to

optimize RE oxide coatings based on specific RE oxide cost, nanocrystallite size and morphology. In this investigation, this optimization was done in the form of simultaneous addition of two different RE oxides. This paper presents: (a) the effect of surface addition of nanocrystalline oxides of different REs on the cyclic oxidation behavior of Fe20Cr alloy and (b) the effect of addition of mixture of two RE oxides, cerium dioxide and lanthanum oxide, on the oxidation behavior of Fe20Cr and Fe20Cr5Al alloys.

2. Methods and Materials

RE oxide sols were prepared as aqueous dispersions of the respective RE oxides with nitric acid, and a non-ionic surfactant. The solution was heated to 80 °C under constant agitation for an hour and the sol formed as sediment. Fe20Cr alloy specimens (1.0 x 1.0 x 0.5 cm) were ground to 400 mesh, rinsed, dried and spray coated with the different RE oxide sols. The specimens were then heated to 150 °C to form a 10 µm thick surface layer of the RE oxide gel. The crystallite sizes of the different RE oxides were determined by x-ray diffraction analysis.

Two sets of experiments were carried out. In the first set, the effect of different RE oxide coats (La_2O_3, CeO_2, Pr_2O_3, Nd_2O_3, Sm_2O_3, Gd_2O_3, Dy_2O_3, Y_2O_3, Er_2O_3, and Yb_2O_3) on cyclic oxidation behavior of Fe-20Cr alloy specimens 1.0 x 1.0 x 0.5 cm was studied. Each oxidation cycle consisted of 2 hours at 900°C. The specimens were weighed after each cycle and oxide spalling marked the end of the test. In the second set of experiments Fe20Cr and Fe20Cr5Al alloy specimens (approximate dimensions 2 x 2 x 3 mm) were coated with CeO_2, La_2O_3 and $CeO_2 + La_2O_3$ and the specimens were isothermally oxidized at 1000° C for about 400 minutes in a thermal balance. The weight gain per unit area versus time curves was plotted. The surfaces of all the specimens were examined in a scanning electron microscope (SEM) coupled to an energy dispersive spectroscopy (EDS) system. The oxide scales were also analyzed by x-ray diffraction (XRD) analysis.

3. Results and Discussion

The morphology of the RE oxide gels are shown in figure 1 and the main morphological features and the crystallite sizes of the RE oxides are given in Table 1. Marked differences in morphology of the oxides can be seen. The results of the first set of experiments are shown in Figure 2. The weight gain of the uncoated and RE oxide coated specimens during oxidation is due to formation of Cr_2O_3 on the specimen surfaces as reported previously by Fernandes and Ramanathan (2000, 2006). The uncoated specimen was cycled five times before the oxide scale spalled. The RE oxide coated specimens were cycled many more times, indicating increased cyclic oxidation resistance (COR) and this varied with the RE oxide on the specimen surface. The chromium dioxide layer on specimens coated with La and Pr oxides did not spall even after 15 cycles. The weight gains of these specimens after one cycle and after 15 cycles were low and about 0.17 mg.cm^{-2}. In general, spalling of the chromium dioxide layer occurred when weight gains exceeded 1.25-1.5 mg.cm^{-2}. This indicated that the time at temperature to reach a specific chromium dioxide layer thickness varied with the nature of RE. The COR of the Fe20Cr alloy coated with the different RE oxides is shown in Table 2. Comparison of data in Tables 1 and 2 reveals two correlations. (a) Between the morphology of the RE oxide and the COR of the specimen coated with that RE oxide. Specimens coated with RE oxides with cube, rod or needle-like morphology withstood a higher number of oxidation cycles compared to those coated with RE oxides with platelet or cluster morphology. (b) Between crystallite size and COR. Except for La_2O_3, the COR of specimens coated with RE oxides (Ce, Pr, Nd, Sm) with crystallite size in the range 58-63 nm was almost double that of specimens coated with RE oxides with crystallite sizes that were almost half that of the cited RE and in the range 25-35 nm (Gd, Dy, Y, Er, Yb). That is, RE oxide with small crystallite size were not as effective as RE oxides with larger crystallite size on COR of Fe20Cr alloy.
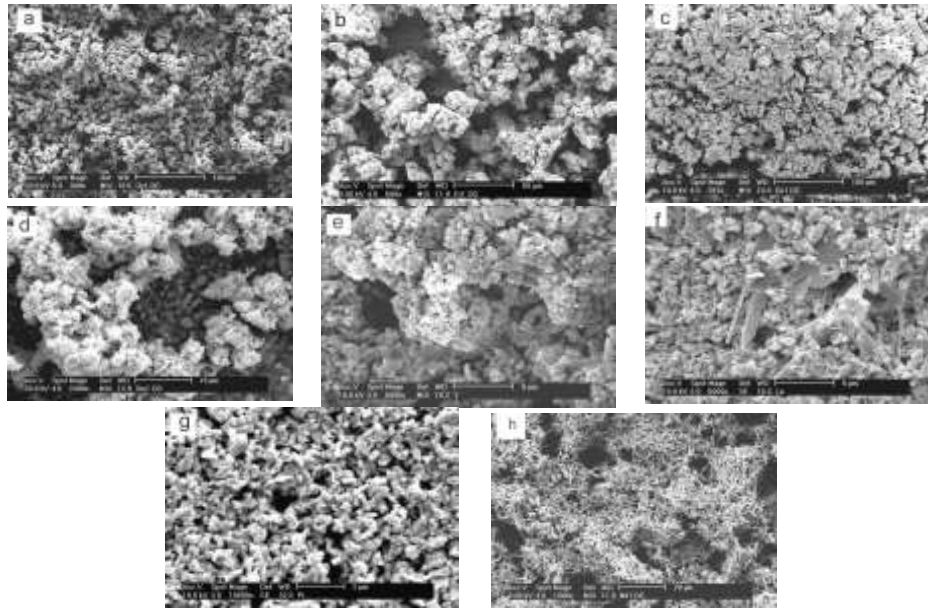
Fig. 1. Scanning electron micrographs of different RE oxides. (a) Dy, (b) Er, (c) Ce, (d) Sm, (e) Y, (f) La, (g) Pr, (h) Nd.

Table 1. Main morphological feature of the rare earth oxides and their crystallite sizes.

| Rare earth oxide	Main morphological feature	Crystallite size(nm)
Lanthanum	Cubes and rods	36.4
Cerium	Cubes	58.4
Praseodymium	Cuboids	60.2
Neodymium	Fine needles, acicular	58.1
Samarium	Clusters	63.0
Gadolinium	Interlocking clusters	27.8
Dysprosium	Tiny clusters	36.6
Yttrium	Platelets	26.9
Erbium	Open clusters	36.6
Ytterbium	Clusters and disperse platelets	26.5
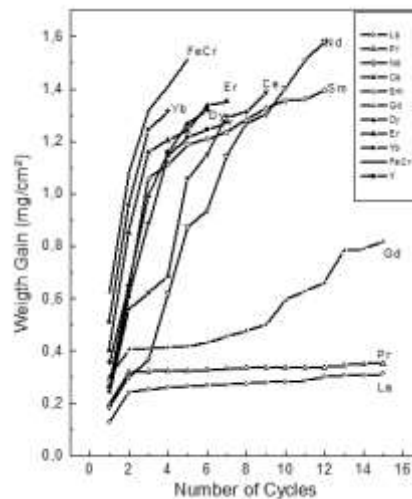
Fig. 2. Weight gain versus number of cycles of oxidation of Fe-20Cr alloy without and with surface deposited RE oxide.

Considering the: (a) low cost and moderate influence of CeO_2 on oxidation resistance of Fe20Cr alloy; (b) marked influence of La_2O_3 and Pr_2O_3 on COR of the same alloy; (c) role of rare earth ion radius; (d) influence of RE oxide morphology; (e) influence of RE oxide crystallite size, the second set of investigations were undertaken to optimize the use of RE oxide coatings to increase oxidation resistance of Fe-Cr alloy. The first step was therefore to evaluate the effect of simultaneous addition of two different RE oxides.

Table 2. Cyclic oxidation resistance of RE oxide coated Fe20Cr alloy, expressed as the number of cycles of oxidation to spalling and the ratios of the RE ion radius to the radius of chromium ion.

Oxide of	Number of cycles at spall	R_{RE}/R_{Cr} ratio
Lanthanum	15+	1.64
Cerium	9	1.60
Praseodymium	15+	1.57
Neodymium	12	1.54
Samarium	12	1.50
Gadolinium	15+	1.46
Dysprosium	6	1.42
Yttrium	7	1.39
Erbium	7	1.37
Ytterbium	4	1.34
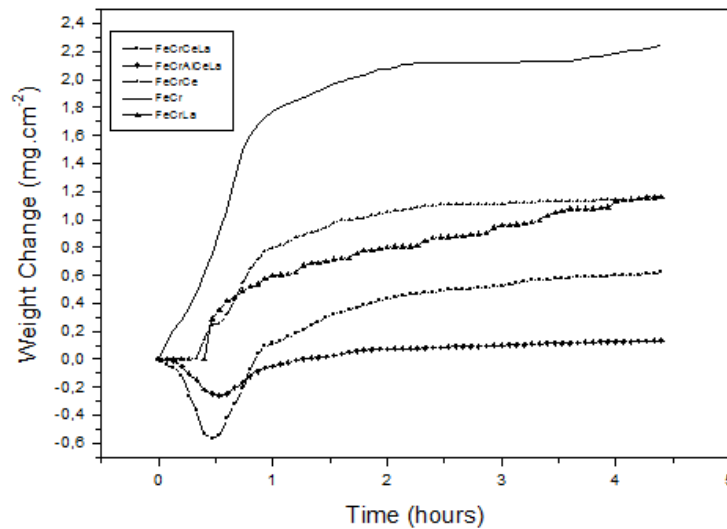
Fig. 3. Isothermal oxidation curves of uncoated, CeO_2 coated, La_2O_3 coated and $CeO_2 + La_2O_3$ coated Fe20Cr as well as $CeO_2 + La_2O_3$ coated Fe20Cr5Al at 1000 °C.

The isothermal oxidation curves of uncoated Fe20Cr, CeO_2 coated Fe20Cr, La_2O_3 coated Fe20Cr, $CeO_2 + La_2O_3$ coated Fe20Cr and $CeO_2 + La_2O_3$ coated Fe20Cr5Al specimens, from the second set of experiments are shown in figure 3. The weight gains of the uncoated and RE oxide coated Fe20Cr and Fe20Cr5Al specimens during oxidation are due to formation of Cr_2O_3 and Al_2O_3 respectively on the specimen surfaces. The chromium dioxide layer on both the uncoated and RE oxide coated Fe20Cr specimens as well as the alumina layer on the Fe20Cr5Al specimens did not spall. All the specimens revealed parabolic oxidation behavior. The effect of rare earth oxide addition to the surface of the Fe20Cr alloy was clearly evident upon comparison of the curves of Fe20Cr and the other RE oxide covered Fe20Cr specimens. Substitution of CeO_2 with La_2O_3 showed some improvement in oxidation behavior. However, when the two oxides CeO_2 and La_2O_3 were jointly present on the surface, the improvement in

oxidation resistance was significant. The curve of the Fe20Cr5Al specimen indicated even higher oxidation resistance. This could be attributed to the joint effect of the low oxidation rate of alumina forming alloys and the effect of the rare earth ion on alumina formation. Work is ongoing to separate these two effects.

4. General Discussion

In the initial or transient stage of oxidation, metastable oxides of base metals such as iron oxide, form on the alloy surface. The effects of RE on scale growth are not evident at this stage. Some of the REs exercise greater influence than others as shown previously by Fernandes and Ramanathan (2006). In the absence of RE in the alloy or on the surface, the new oxide scale grows at the oxide /oxygen interface and in the presence of RE it grows at the metal/oxide interface.

The number of cycles to spalling of the scale on specimens coated with the various RE oxides and the ratio of the radius of the RE ion to the radius of the chromium ion (R_{RE}/R_{Cr}) are shown in Table 2. It is evident that specimens coated with RE oxides that had R_{RE}/R_{Cr} ratios lower than 1.45 withstood only half as many cycles compared with those coated with RE oxides that had R_{RE}/R_{Cr} ratios higher than 1.45. The crystallite size and morphology of the different RE oxide revealed marked differences as reported by Hou and Stringer (1987) and Fernandes and Ramanathan (2006). The COR of Fe-20Cr alloy coated with RE oxide varied and it was shown that COR depends on the thickness of the chromium dioxide layer formed on the alloy surface. In the presence of an RE oxide coating the chromium dioxide layer formed after the first cycle of oxidation is thinner than that on surfaces without a RE oxide coating and it varied with RE oxide. Spalling of the chromium dioxide layer, which marks the breakdown of COR, occurs when its thickness reaches a critical value. Hence, the longer it takes to reach this critical oxide scale thickness, higher the COR. Characteristics of the RE oxide coating that affect the time required to reach this critical oxide scale thickness are the ionic radii of the RE, the shape and size of the RE oxide crystallites and the coverage.

4.1. Role of Rare Earths in Improving H.T. Oxidation Resistance of Chromium Dioxide Forming Alloys

During oxidation of RE containing alloys the RE diffuse into the scale due to the oxygen potential gradient which extends from the gas interface into the substrate. In the case of the RE oxide coated alloys, the coating gets incorporated in the growing scale as shown previously by Fernandes and Ramanathan (2000). Both in the RE element containing alloy's surface oxide and RE oxide coated alloy's oxide the RE diffuses through the oxide to the gas interface. Proof of this was shown after prolonged oxidations by Pint (1996). The RE ions first segregate to the metal-scale interface and then follow the fastest path to the gas interface, which are the scale grain boundaries as shown previously by Cotell et.al. (1990) and Pint et.al. (1995). When the RE ion concentration at the grain boundaries reaches a critical amount it results in the two effects that have been observed in this study.

The first effect is inhibition of normal outward short-circuit transport of alloy cations along the scale grain boundaries due to the slower diffusion of the large RE ions. It is also probable that RE with higher ionic radius diffuse slower along the grain boundaries compared with the RE ion with a smaller radius. Hence, bigger the RE ion, higher is the inhibition of alloy cation transport. The higher COR of Fe20Cr coated with La_2O_3, compared with that coated with Pr_2O_3, or any other RE oxide is further proof of the effect of the RE ion size. In this case the time taken to form the critical chromia layer thickness is significantly longer. During much of this period, the scale formed is thin, more plastic, more adherent to the alloy and therefore capable of withstanding stresses associated with scale growth and temperature cycling. Similar observations were reported previously by Papaiacovou and Hussey (1990) with respect to scale growth on ceria coated Fe-Cr alloys. Direct correlation between RE ion radius and cyclic oxidation resistance has been found. As a result, the new rate-limiting step is the inward transport of O^- ions along the scale grain boundaries.

The second effect is reduction in scale grain growth and this is due a solute-drag effect of the RE ions on the scale grain boundaries as shown by Kingery (1976). This results in a smaller average grain size in α-Cr_2O_3 scales and higher scale plasticity as noted by Ramnarayanan et.al. (1984).

5. Conclusions

1. The cyclic oxidation resistance (COR) of nanocrystalline RE oxide coated Fe-20Cr alloy was significantly higher than that of the uncoated alloy.
2. Correlations between RE ion radius as well as RE oxide crystallite size and oxidation resistance of chromia forming Fe-20Cr alloy have been observed.
3. The oxidation resistance of Fe-20Cr coated with La_2O_3 was higher than that of the same alloy coated with CeO_2.
4. The oxidation resistance of Fe-20Cr coated with CeO_2 and La_2O_3 was even higher than that of the same alloy coated with either RE oxide and attributed to optimization in RE oxide grain size and shape, consequent increase in coverage and also to optimization in the chemical potentials of two REO with ionic radii very close to one another.
5. The oxidation resistance of the Al containing alloy coated with a mixture of CeO_2 and La_2O_3 was even higher.

References

Stott, F.H. Influence of alloy additions on oxidation. (1989) Materials Science and Technology, 5, 734-740.

Stringer, J. (1989) The reactive elements effect in high temperature corrosion. Materials Science and Engineering, A120, 129-137.

Hou, P.Y., Stringer, J. (1987) The effect of surface applied reactive metal oxide on the high temperature oxidation of alloys. Materials Science and Engineering, 87, 295-302.

Ramanathan, L.V. (1993) Role of rare earth elements on high temperature oxidation behavior of Fe-Cr, Ni-Cr and Ni-Cr-Al alloys. Corrosion Science, 35 (5-8), 871-878.

Seal, S., Roy, S.K., Bose S.K., Kuiry S.C. (2000) Ceria based high temperature coatings for oxidation prevention. Journal of Materials, 52.1.

Bennet, M.J. (1984) New coatings for high temperature materials protection. Journal of Vacuum Science and Technology, B2 (4), 800-805.

Fernandes, S.M.C., Ramanathan, L.V. (2000) Influence of rare earth oxide coatings on oxidation behavior of Fe-20Cr alloys. Surface Engineering, 16 (4), 327-332.

Fernandes, S.M.C., Ramanathan, L.V. (2006) Effect of surface deposited rare earth oxide gel characteristics on cyclic oxidation behavior of Fe20-Cr alloys. Materials Research, 9, 199-203.

Pint, B. (1996) Experimental observations in support of the dynamic-segregation theory to explain the reactive-element effect. Oxidation of Metals, 45, 1.

Cotell, C.M., Yurek, G.J., Hussey, R.J., Mitchell, D.F., GRAHAM, M.J. (1990) The influence of grain boundary segregation of yttrium in chromium dioxide on the oxidation of chromium metal. Oxidation of Metals, 34, 173-216.

Pint, B., Garratt-Reed, A.J.; Hobbs, L.W. (1995) The reactive element effect in ODS FeCrAl alloys, Materials at High temperatures, 13, 3-16.

Papaiacovou, P., Hussey, R.J. (1990) The effect of CeO_2 coatings on the oxidation behavior of Fe-20Cr alloys in O_2 at 1173K. Corrosion Science, 30(4/5), 451-460.

Kingery, W.D., Bowen, H.K., Uhlmann, D.R. (1976) Introduction to ceramics, Wiley, New York.

Ramnarayanan, T.A., Raghavan, M.; Petkovic-Luton, R. (1984) The Characteristics of alumina scales formed on Fe-based yttria-dispersed alloys, Journal of Electrochemical Society, 131, 923.